

Weighted residual estimators for a posteriori estimation of pointwise gradient errors in quasilinear elliptic problems

Alan Demlow*

Abteilung für Angewandte Mathematik, Hermann-Herder-Str. 10, 79104 Freiburg, Germany. e-mail: demlow@mathematik.uni-freiburg.de

The date of receipt and acceptance will be inserted by the editor

Summary We present a weighted residual scheme for estimation of pointwise gradient errors in finite element methods for quasilinear elliptic problems. First we define computable residual weights which may be conveniently determined using local ellipticity properties of the underlying differential operator. Using a combination of theoretical and computational results, the resulting a posteriori error estimator is shown to bound the error up to nonessential constants and higher-order terms. Further properties of this estimator are investigated and illustrated using computational experiments.

Key words Finite element methods, quasilinear elliptic problems, a posteriori error estimation, pointwise error analysis

Mathematics Subject Classification (1991): 65N30, 65N15

1 Introduction

We consider finite element approximations to second-order quasilinear elliptic Dirichlet boundary value problems having the form

$$\begin{aligned} -\sum_{i=1}^n \frac{\partial}{\partial x_i} F_i(x, \nabla u) &= f(x) \text{ in } \Omega, \\ u &= 0 \text{ on } \partial\Omega. \end{aligned} \tag{1.1}$$

Here $\Omega \subset \mathbb{R}^n$, $n \geq 2$, is a bounded domain whose boundary $\partial\Omega$ is sufficiently regular to ensure that $u \in C^{1,\alpha}(\overline{\Omega})$ for some $\alpha > 0$.

* This material is based upon work supported under a grant of the Deutsche Forschungsgemeinschaft.

In order to avoid technicalities arising from finite element approximations on domains with smooth boundaries, we shall also assume throughout that Ω is convex and polyhedral. Smooth boundaries are in principle admissible if appropriate modifications are made. The vector $\mathbf{F} = \{F_i\}_{i=1,\dots,n}$ of coefficients is assumed to be sufficiently smooth and to satisfy the ellipticity condition

$$0 < \lambda(x, p)|\xi|^2 \leq \sum_{i,j=1}^n F_{ij}(x, p)\xi_i\xi_j \leq \Lambda(x, p)|\xi|^2$$

for all $x \in \overline{\Omega}$ and $p, \xi \in \mathbb{R}^n$. Here $F_{ij}(x, p) = \frac{\partial}{\partial p_j} F_i(x, p)$. Finally, we assume that the matrix $[F_{ij}(x, p)]$ is symmetric for $(x, p) \in \Omega \times \mathbb{R}^n$. Two examples of problems satisfying these conditions are uniformly elliptic linear problems where $\mathbf{F}(x, p) = A(x)p$ and the highly nonlinear and nonuniformly elliptic prescribed mean curvature equation, where $\mathbf{F}(x, p) = p/\sqrt{1 + |p|^2}$.

Residual-based error estimates for finite element methods are used widely in a posteriori error estimation and adaptive mesh refinement. However, the effects of the ellipticity properties of the Hessian matrix $A(x) = [F_{ij}(x, \nabla u(x))]$ on residual estimators have only recently been studied even in the context of the energy and similar norms. These ellipticity properties must be explicitly taken into account when using such estimators or the accuracy of the resulting a posteriori upper bound degenerates if the eigenvalues of A differ much from 1. For the energy or similar norms, the residual indicator for a given element should be weighted by an appropriate power of the smallest eigenvalue of A (or its discrete counterpart in nonlinear problems) on that element; cf. [7] and [6]. However, if the maximum pointwise ratio of the largest and smallest eigenvalues of A is large, a considerable “eigenvalue gap” develops between the a posteriori upper and lower bounds given by residual estimators even if the elementwise residuals are appropriately weighted (cf. [7] and [1]).

Residual-based a posteriori error estimates for pointwise gradient errors in finite element methods for the equation (1.1) were proved in [4]. Let u_h be a continuous piecewise polynomial finite element approximation to u on a simplicial grid. Then one may easily slightly sharpen and extend the results of [4] to finite element spaces of arbitrary polynomial degree to obtain the global a posteriori upper bound

$$\|\nabla(u - u_h)\|_{L^\infty(\Omega)} \leq C_1 \ell_h \max_{T \in \mathcal{T}} \mathcal{E}_T + R_2(\Omega) \quad (1.2)$$

and local a posteriori lower bound

$$\frac{1}{\|A^h\|_{L^\infty(S_T)}} \mathcal{E}_T \leq C \|\nabla(u - u_h)\|_{L^\infty(S_T)} + R_1(S_T). \quad (1.3)$$

Here A^h is the largest eigenvalue of $[F_{ij}(\cdot, \nabla u_h)]$, \mathcal{E}_T is a first-order maximum norm residual on an element T in a simplicial decomposition \mathcal{T} of Ω , and S_T is a small mesh patch about T . Also, R and R_i denote terms generically of higher order, and ℓ_h is a logarithmic factor of the smallest mesh diameter. The reliability constant C_1 depends on the domain Ω and *global* ellipticity and weak continuity properties (Dini-continuity) of the coefficient matrix A . Computational experiments indicate that not only does C_1 blow up as the smallest eigenvalue of A decreases to 0, but that the effectiveness of the local residual \mathcal{E}_T as an elementwise error indicator for use in adaptive mesh refinement generally degenerates as well. Thus the constant C_1 must in a sense be estimated locally in order to yield an effective a posteriori error indicator.

In this paper we more precisely study the effects of the ellipticity properties of A on residual a posteriori error estimates for pointwise gradient errors when the space dimension $n = 2$ and propose a weighted residual scheme which takes ellipticity properties into account in a local and computable fashion. First we define a residual estimator for $\|\nabla(u - u_h)\|_{L^\infty(\Omega)}$ which has the form $\max_{T \in \mathcal{T}} W(T) \mathcal{E}_T$. The residual weight $W(T)$ is computable a posteriori and depends in a dual sense on the ellipticity properties of the discrete Hessian matrix $[F_{ij}(\cdot, \nabla u_h)]$ *locally* on the element T . We prove that $\|\nabla(u - u_h)\|_{L^\infty(\Omega)}$ is bounded up to higher-order terms and constants not depending on A or other essential quantities by a weighted residual estimator with weights which are not computable a posteriori but which are closely related to $W(T)$. Starting with these theoretical results, the use of $W(T)$ is then justified by computational and heuristic arguments. As when using residual estimators for energy norms, there is a considerable and practically significant gap between the a posteriori upper error estimator $\max_{T \in \mathcal{T}} W(T) \mathcal{E}_T$ and the lower bound given in (1.3) when the maximum pointwise ratio of the eigenvalues of A is large. Test computations show that both the upper and lower bounds we obtain are sharp up to higher-order terms.

An outline of the paper is as follows. In §2 we give definitions and some preliminary lemmas. In §3 we define the weight $W(T)$ for space dimension $n = 2$ and discuss its properties. In §4 we state and prove theoretical results which are valid for arbitrary space dimension $n \geq 2$, argue that the weight $W(T)$ bounds the weights in our rigorous

estimate up to a logarithmic factor, and discuss the properties of the resulting a posteriori estimate. Finally, in §5 we provide numerical examples illustrating both the utility of the weighted residual estimator $\max_{T \in \mathcal{T}} W(T) \mathcal{E}_T$ and also the negative consequences of the “eigenvalue gap” between $W(T)$ and the lower residual weight $\frac{1}{\|A^h\|_{L^\infty(T)}}$ from (1.3) in linear and nonlinear test problems.

2 Preliminaries

In this section we make a number of definitions and state some lemmas. Here we assume that the space dimension $n \geq 2$ as our theoretical results are valid for arbitrary space dimension.

2.1 Finite element approximation and mesh

Let $h_T = |T|^{\frac{1}{n}}$. We assume that \mathcal{T} is a shape-regular simplicial decomposition of Ω , that is, that each element $T \in \mathcal{T}$ contains a sphere of radius $\tilde{c}h_T$ and is contained in a sphere of radius $\tilde{C}h_T$. No further restrictions are placed on \mathcal{T} , so that highly graded and unstructured meshes are admitted. For $D \subset \Omega$, let $\mathcal{T}_D = \{T \in \mathcal{T} : T \cap D \neq \emptyset\}$ and $D^h = \text{interior}(\cup_{T \in \mathcal{T}_D} \bar{T})$. Also, let $\underline{h} = \min_{T \in \mathcal{T}} h_T$, and $\bar{h} = \max_{T \in \mathcal{T}} h_T$. Letting T_x be an arbitrary element whose closure contains the point x , we denote by $h(x)$ the quantity h_{T_x} . In addition, let P_T denote the patch of elements sharing a vertex with T and let S_T denote the star of elements sharing a face with T . Let S_h^r be a space of continuous piecewise polynomials of degree $r - 1$ which are 0 on $\partial\Omega$, and let $u_h \in S_h^r$ satisfy

$$\int_{\Omega} \mathbf{F}(x, \nabla u_h) \cdot \nabla \chi \, dx = \int_{\Omega} f \chi \, dx \quad \forall \chi \in S_h^r.$$

Next let S be a face which is shared by two elements T_1 and T_2 and which has unit normal \mathbf{n} . For $x \in S$, let $[\mathbf{F}(x, \nabla v_h)](x) = (\mathbf{F}(x, \nabla v_h|_{T_1}) - \mathbf{F}(x, \nabla v_h|_{T_2})) \cdot \mathbf{n}$. We then define the first-order elementwise maximum norm residual

$$\mathcal{E}_T = h_T \|f + \operatorname{div} \mathbf{F}(\cdot, \nabla u_h)\|_{L^\infty(T)} + \|[\mathbf{F}(\cdot, \nabla u_h)]\|_{L^\infty(\partial T)}.$$

We shall employ the Scott-Zhang interpolant $I_h : W_1^1(\Omega) \rightarrow S_h^r$ defined in [14] which preserves homogeneous boundary conditions and which for $1 \leq p \leq \infty$ satisfies

$$\|v - I_h v\|_{L_p(T)} \lesssim h_T^j |v|_{W_p^j(P_T)}, \quad 1 \leq j \leq r, \quad (2.1)$$

and

$$\|v - I_h v\|_{W_p^1(T)} \lesssim h_T^j |v|_{W_p^{j+1}(P_T)}, \quad 0 \leq j \leq r-1. \quad (2.2)$$

Here and throughout $a \lesssim b$ means that $a \leq Cb$, where C depends only on nonessential quantities. We shall actually apply I_h in a slightly modified form. Assume that $v \in H_0^1(D)$ for some fixed subset D of Ω . We may define I_h so that

$$\text{supp}(I_h v) \subset \overline{D^h}. \quad (2.3)$$

Indeed, doing so only requires that for each nodal point $a_i \in \partial D^h$, the face associated to a_i in [14] does not lie in the interior of D^h , a choice which may be made in the definition of I_h . I_h then depends on D , but the constants hidden in “ \lesssim ” in (2.1) and (2.2) do not.

2.2 Auxiliary problems and assumptions on coefficients

First we define shorthand notation for the eigenvalues of $A(x) = [F_{ij}(x, \nabla u)]$ and $[F_{ij}(x, \nabla u_h)]$. Let $\lambda(x)$ and $\lambda^h(x)$ be the smallest eigenvalues of $[F_{ij}(x, \nabla u)]$ and $[F_{ij}(x, \nabla u_h)]$, respectively, and let $\Lambda(x)$ and $\Lambda^h(x)$ be the corresponding largest eigenvalues. For $D \subset \Omega$, we also define $\Lambda_D = \max_{x \in D} \Lambda(x)$, $\lambda_D = \min_{x \in D} \lambda(x)$, $\lambda_D^h = \min_{x \in D} \lambda^h(x)$, and $\Lambda_D^h = \max_{x \in D} \Lambda^h(x)$.

We assume that the coefficients $F_i(x, p)$ are twice continuously differentiable in p . Recalling the definition $F_{ij}(x, p) = \frac{\partial}{\partial p_j} F_i(x, p)$, we similarly let $F_{ijk}(x, p) = \frac{\partial^2}{\partial p_j \partial p_k} F_i(x, p)$. We also require that $\mathbf{F}(x, p)$ has first derivatives with respect to the x variable which are uniformly bounded with respect to both x and p .

Several auxiliary bilinear forms are used in our analysis of quasi-linear problems. Following for example [8] we first define

$$a_{ij}^h = \int_0^1 F_{ij}(x, \nabla u_h + t \nabla(u - u_h)) dt, \quad i, j = 1, \dots, n$$

and

$$A_h(v, w) = \int_{\Omega} \sum_{i,j=1}^n a_{ij}^h v_{x_j} w_{x_i} dx. \quad (2.4)$$

For $v \in H_0^1(\Omega)$ and $\chi \in S_h^r$,

$$\begin{aligned} A_h(u - u_h, v) &= \int_{\Omega} \sum_{i=1}^n (\mathbf{F}(x, \nabla u) - \mathbf{F}(x, \nabla u_h)) \cdot \nabla v dx \\ &= \int_{\Omega} \sum_{i=1}^n (\mathbf{F}(x, \nabla u) - \mathbf{F}(x, \nabla u_h)) \cdot \nabla(v - \chi) dx \\ &= A_h(u - u_h, v - \chi). \end{aligned} \quad (2.5)$$

Letting $a_{ij} = F_{ij}(x, \nabla u)$, $i, j = 1, \dots, n$, we next define

$$A(v, w) = \int_{\Omega} \sum_{i,j=1}^n a_{ij} v_{x_j} w_{x_i} dx.$$

We finally define two forms with constant coefficients,

$$A_h^{x_0}(v, w) = \int_{\Omega} \sum_{i,j=1}^n F_{ij}(x_0, \nabla u_h(x_0)) v_{x_j} w_{x_i} dx$$

and

$$A^{x_0}(v, w) = \int_{\Omega} \sum_{i,j=1}^n F_{ij}(x_0, \nabla u(x_0)) v_{x_j} w_{x_i} dx.$$

Abusing notation slightly, we shall at times let A_h refer to the matrix $[a_{ij}^h]$ as well as to the associated bilinear form, and similarly with A , $A_h^{x_0}$, and A^{x_0} .

Several relationships between A , A_h , $A_h^{x_0}$, and A^{x_0} will play an important role in the subsequent analysis. We sum these relationships up in the following elementary lemma.

Lemma 2.1 *Assume that $D \subset \Omega$ and $v, w \in H_0^1(\Omega)$ with $\text{supp}(v) \cap \text{supp}(w) \subset D$. Assume that either $\|\nabla u_h\|_{L^\infty(\Omega)} \lesssim 1 + \|\nabla u\|_{L^\infty(\Omega)}$ or that for $1 \leq i, j, k, \leq n$, $\|F_{ijk}\|_{L^\infty(\Omega \times \mathbb{R}^n)} \lesssim 1$. Then for any $x_0 \in D$,*

$$\begin{aligned} |(A_h^{x_0} - A_h)(v, w)| \\ \lesssim [C_F \|\nabla(u - u_h)\|_{L^\infty(D)} + \text{diam}(D) |A|_{C^{0,\alpha}(\bar{D})}] \\ \cdot \|\nabla v\|_{L^\infty(D)} \|\nabla w\|_{L^1(D)}, \end{aligned} \quad (2.6)$$

where C_F depends on \mathbf{F} and $\|\nabla u\|_{L^\infty(\Omega)}$.

Proof. First note that

$$\begin{aligned} |(A_h^{x_0} - A_h)(v, w)| \leq |(A_h^{x_0} - A^{x_0})(v, w)| + |(A^{x_0} - A)(v, w)| \\ + |(A - A_h)(v, w)|. \end{aligned} \quad (2.7)$$

With S denoting the convex hull of $\text{range}(\nabla u)$ and $\text{range}(\nabla u_h)$, we next compute

$$\begin{aligned} |a_{ji} - a_{ji}^h| &= \left| \int_0^1 F_{ji}(\nabla u) - F_{ji}(\nabla u_h + t\nabla(u - u_h)) dt \right| \\ &\leq \int_0^1 \sum_{k=1}^n \|F_{jik}\|_{L^\infty(S)} (1-t) |\nabla(u - u_h)_k| dt \\ &\leq C_F |\nabla(u - u_h)|, \end{aligned} \quad (2.8)$$

and similarly,

$$|F_{ij}(x_0, \nabla u(x_0)) - F_{ij}(x_0, \nabla u_h(x_0))| \leq C_F |\nabla(u - u_h)(x_0)|. \quad (2.9)$$

The essential estimate $\max_{1 \leq i, j, k \leq n} \|F_{ijk}\|_{L_\infty(S)} \leq C_F$ may be established here in one of two ways. If F_{ijk} is bounded on $\Omega \times \mathbb{R}^n$, the bound is immediate and does not rely on ∇u and ∇u_h . If alternatively $\|\nabla u_h\|_{L_\infty(\Omega)} \lesssim 1 + \|\nabla u\|_{L_\infty(\Omega)}$ (which holds if for example $\|\nabla(u - u_h)\|_{L_\infty(\Omega)} \lesssim 1$), C_F can then be taken to be the bound for $\max_{1 \leq i, j, k \leq n} |F_{ijk}(x, p)|$ on the compact set $\{x \in \bar{\Omega}, |p| \lesssim 1 + \|\nabla u\|_{L_\infty(\Omega)}\}$. Noting that

$$\begin{aligned} & |(A^{x_0} - A)(v, w)| \\ & \lesssim \max_{1 \leq i, j \leq n} \|a_{ij} - a_{ij}(x_0)\|_{L_\infty(D)} \|\nabla v\|_{L_1(D)} \|\nabla w\|_{L_\infty(D)} \\ & \lesssim \text{diam}(D) \|A\|_{C^{0,\alpha}(\bar{D})} \|\nabla v\|_{L_\infty(D)} \|\nabla w\|_{L_1(D)} \end{aligned}$$

and inserting the above inequality along with (2.8) and (2.9) into (2.7) while applying Hölder's inequality completes the proof of (2.6). \square

2.3 Special subdomains

In our arguments we shall need to carry out duality arguments on subdomains whose size and shape (regularity properties) we can both control. These subdomains will be polyhedra of fixed shape and with size equivalent to d . We associate to each point $x \in \Omega$ and each d with $0 < d < 1$ a subdomain $D_d(x) \subset \Omega$ with the following properties:

1. $x \in D_d(x)$.
2. $D_d(x)$ is a copy of a fixed convex polyhedral domain $\tilde{\Omega}$ which is scaled by d and translated.
3. There exists a smooth cutoff function ω such that $\omega \equiv 1$ on T_x , $0 \leq \omega \leq 1$, $\|D^j \omega\|_{L_\infty(\Omega)} \leq Cd^{-j}$ ($j = 0, 1, 2$), and $\omega \equiv 0$ on $\Omega \setminus D_d(x)$. Equivalently, there exists $k > 0$ which depends at most on Ω such that $\text{dist}(x, \partial D_d(x) \setminus \partial \Omega) \geq kd$.
4. $\text{dist}(\text{supp}(\omega), \partial D_d(x) \setminus \partial \Omega) > 0$, and $\cup_{T \in \mathcal{T}_{\text{supp}(\omega)}} T \subset D_d(x)$.

It is straightforward to verify that one may find such subdomains $D_d(x)$ for convex polygons Ω ; indeed, we may simply let $D_d(x)$ be a scaled copy of Ω . However, the choice of the special subdomain $D_d(x)$ will also have practical significance in the definition of our elementwise residual weights $W(T)$. Later we shall define the weight $W(T)$ by solving a dual problem on $\tilde{\Omega}$. It is in certain cases advantageous to solve this dual problem on $\tilde{\Omega} \neq \Omega$. For example, in this work we give values of $W(T)$ when Ω is a unit square, and we choose $\tilde{\Omega} = \Omega$. If we wanted to instead compute on a rectangular domain we could still take $\tilde{\Omega}$ to be a square and thus employ the same weights as when Ω is a square.

2.4 Green's function estimates

Let $G(x, y)$ denote a Green's function satisfying $\int_{\bar{\Omega}} A_h^{x_0} \nabla_y G(x, y) \cdot \nabla v(y) dy = v(x)$ for sufficiently smooth $v \in H_0^1(\bar{\Omega})$ and for some $x_0 \in \Omega$. The following estimate for the first and mixed second derivatives of G is essential to our proofs.

Lemma 2.2 *Assume that $\partial\Omega$ is smooth or Ω is convex, that $|\alpha| \leq 1$ and $|\beta| \leq 1$, and that $\|\nabla u_h\|_{L_\infty(\Omega)} \lesssim 1 + \|\nabla u\|_{L_\infty(\Omega)}$. Then for $n \geq 3$,*

$$|D_x^\alpha D_y^\beta G(x, y)| \leq C_G |x - y|^{2-n-|\alpha|-|\beta|}, \quad (2.10)$$

and for $n = 2$

$$|D_x^\alpha D_y^\beta G(x, y)| \leq C_G |x - y|^{2-n-|\alpha|-|\beta|} \log \frac{1}{|x - y|}. \quad (2.11)$$

Here C_G depends on Ω , \mathbf{F} , and $\|\nabla u\|_{L_\infty(\Omega)}$.

The estimate (2.10) for space dimension $n \geq 3$ may be found in [10] assuming that $\partial\Omega$ satisfies a uniform exterior sphere condition. This condition is met by both convex and smooth domains. The proof given in [10] does not carry directly over to $n = 2$ due to the logarithmic nature of the singularity, but one may use the same method to obtain the suboptimal estimate (2.11) so long as the estimate $|G(x, y)| \leq C \log \frac{1}{|x-y|}$ is known. This estimate is contained in [5] under the weak restrictions of L_∞ and uniformly elliptic coefficients and Lipschitz boundary $\partial\Omega$. Also note that since the coefficients of the bilinear form $A_h^{x_0}$ are constant, C_G only depends on ellipticity properties of $A_h^{x_0} = [F_{ij}(x_0, \nabla u_h)]$ which in turn rely only on \mathbf{F} and $\|\nabla u\|_{L_\infty(\Omega)}$ since $\|\nabla u_h\|_{L_\infty(\Omega)} \lesssim 1 + \|\nabla u\|_{L_\infty(\Omega)}$.

2.5 Regularized δ -function

As in [4], our proofs here make use of regularized Green's and δ functions. In order to define a regularized δ -distribution, we first let δ_1^0 be a fixed smooth nonnegative function satisfying $\text{supp}(\delta_1^0) \subset B_1(0)$ and $\int_{\mathbb{R}^n} \delta_1^0 dx = 1$. For $\rho > 0$ we then define

$$\delta_\rho^{x_0}(x) = \rho^{-n} \delta_1^0\left(\frac{x - x_0}{\rho}\right)$$

and note that by scaling

$$\|\delta_\rho^{x_0}\|_{W_p^k(\mathbb{R}^n)} \leq C \rho^{-k-n(1-\frac{1}{p})}, \quad 1 \leq p \leq \infty, \quad k = 0, 1.$$

Lemma 2.3 *Let $\chi \in S_h^r$, $T \in \mathcal{T}$, and $u \in C^{1,\alpha}(\bar{T})$. Also let $\rho \leq \min(h_T^2, \frac{1}{4C_T^2})$ with C_T depending only on the shape-regularity of T . Then there exists a unit vector $\boldsymbol{\nu}_T$ and a point $x_T \in T$ such that*

$$\|\nabla(u - \chi)\|_{L_\infty(T)} \lesssim |(u - u_h, \operatorname{div}(\boldsymbol{\nu}_T \delta_\rho^{x_T}))| + \rho^\alpha |u|_{C^{1,\alpha}(\bar{T})},$$

where ∂ denotes the first-order directional derivative defined by $\partial v = \nabla v \cdot \boldsymbol{\nu}_T$.

Proof. Let x_1 and $\boldsymbol{\nu}_T$ be a point in T and a unit vector such that

$$\|\nabla(u - \chi)\|_{L_\infty(T)} \lesssim |\partial(u - \chi)(x_1)|. \quad (2.12)$$

Next let $x_T \in T$ be such that $|x_T - x_1| \lesssim \rho$ and $\operatorname{supp}(\delta_\rho^{x_T}) \subset T$. Note that $\int_T \partial(u - \chi) \delta_\rho^{x_T} dx = \partial(u - \chi)(x_2)$ for some $x_2 \in \operatorname{supp}(\delta_\rho^{x_T})$, and that by the triangle inequality $|x_1 - x_2| \lesssim \rho$. Thus

$$\partial(u - \chi)(x_1) = \partial(u - \chi)(x_1) - \partial(u - \chi)(x_2) + \int_T \partial(u - \chi) \delta_\rho^{x_T} dx. \quad (2.13)$$

But

$$\begin{aligned} |\partial(u - \chi)(x_1) - \partial(u - \chi)(x_2)| &\leq |\partial u(x_1) - \partial u(x_2)| \\ &\quad + |\partial \chi(x_1) - \partial \chi(x_2)| \\ &\lesssim \rho^\alpha |u|_{C^{1,\alpha}(\bar{T})} + \rho |\partial \chi|_{W_\infty^1(T)}. \end{aligned} \quad (2.14)$$

Applying an inverse inequality and recalling that $\rho \leq h_T^2$, we find that

$$\begin{aligned} \rho |\partial \chi|_{W_\infty^1(T)} &= \rho |\partial \chi - \partial u(x_T)|_{W_\infty^1(T)} \\ &\leq C_T \rho h_T^{-1} \|\partial \chi - \partial u(x_T)\|_{L_\infty(T)} \\ &\leq C_T (\sqrt{\rho} \|\partial(u - \chi)\|_{L_\infty(T)} + \rho h_T^{-1} \|\partial u - \partial u(x_T)\|_{L_\infty(T)}) \\ &\leq C_T (\sqrt{\rho} \|\nabla(u - \chi)\|_{L_\infty(T)} + \rho h_T^{\alpha-1} |u|_{C^{1,\alpha}(\bar{T})}). \end{aligned} \quad (2.15)$$

Noting that $\rho h_T^{\alpha-1} = \rho^\alpha \rho^{1-\alpha} h_T^{\alpha-1} \leq \rho^\alpha$ and then combining (2.12) through (2.15), we obtain

$$\begin{aligned} \|\nabla(u - \chi)\|_{L_\infty(T)} &\leq C_T [|\int_T \partial(u - \chi) \delta_\rho^{x_T} dx| \\ &\quad + \rho^\alpha |u|_{C^{1,\alpha}(\bar{T})} + \sqrt{\rho} \|\nabla(u - \chi)\|_{L_\infty(T)}]. \end{aligned}$$

Recalling that $\sqrt{\rho} \leq \frac{1}{2C_T}$ and kicking back the last term above yields the desired result. \square

3 The weight $W(T)$ and its properties

In this section we precisely define the weight $W(T)$ and discuss the gap between a posteriori upper and lower bounds resulting from its use.

3.1 Definition of $W(T)$

In this section we define a computable weighted residual estimator for $\|\nabla(u - u_h)\|_{L^\infty(\Omega)}$, where Ω is now a convex polygonal domain in \mathbb{R}^2 . Let $g^{x_0} \in H_0^1(\Omega)$ solve

$$-\operatorname{div}(\tilde{A}_h^{x_0} g^{x_0}) = \operatorname{div}(\boldsymbol{\nu} \delta_\epsilon^{x_c}) \text{ in } \tilde{\Omega}, \quad (3.1)$$

where $\tilde{A}_h^{x_0}$ is a diagonal matrix with entries $\tilde{a}_{11}^h = \lambda^h(x_0)$ and $\tilde{a}_{22}^h = \Lambda^h(x_0)$ and $\boldsymbol{\nu}$ is a unit vector. g^{x_0} is thus a regularized Green's function which reflects in a dual sense the ellipticity properties induced by the discrete gradient ∇u_h in the equation (1.1) at x_0 . Essentially we shall define $W(T)$ as $\max_{x_0 \in T} \|\nabla g^{x_0}\|_{L_1(\tilde{\Omega})}$.

In order to complete the definition of g^{x_0} , we must fix $\tilde{\Omega}$, $\boldsymbol{\nu}$, and $\delta_\epsilon^{x_c}$. For the sake of concreteness we describe our choices of these parameters for a model computation; the principles involved in choosing them apply in other situations as well. Let then $\Omega = (0, 1)^2$ be the unit square, and let $\tilde{\Omega} = \Omega$. Also let

$$\delta_1^0(x) = \begin{cases} C_\delta e^{\frac{-1}{1-|x|^2}}, & |x| < 1, \\ 0, & |x| \geq 1, \end{cases}$$

where C_δ is taken so that δ_0^1 has unit mass. We fix the point $x_c = (.5, .5)$ and let $\delta_\epsilon^{x_c}(x) = \epsilon^{-2} \delta_0^1(\frac{x-x_c}{\epsilon})$. x_c is chosen as the center-point of Ω because computational experiments indicate that doing so maximizes $\|\nabla g^{x_0}\|_{L_1(\Omega)}$ over possible choices of x_c . The choice of ϵ must be balanced between two extremes. The theory presented in the following section relies on the use of regularized Green's function for which the corresponding radius of support is asymptotically very small. Thus choosing ϵ to be small agrees with our theory. On the other hand, computing g^{x_0} becomes more difficult when ϵ is very small, and both theory and computational experience indicate that $\|\nabla g^{x_0}\|_{L_1(\tilde{\Omega})}$ grows approximately logarithmically with $\frac{1}{\epsilon}$ so that the relative values of $\|\nabla g^{x_0}\|_{L_1(\tilde{\Omega})}$ for different values of λ^h and Λ^h are affected at most moderately by changing ϵ . In our experiments we chose $\epsilon = 10^{-5}$.

It can be argued from our theoretical analysis that the best choice of $\boldsymbol{\nu}$ would be $\nabla(u - u_h)(x_0)/|\nabla(u - u_h)(x_0)|$. As the direction of the error is not available a posteriori we instead choose $\boldsymbol{\nu}$ so as to maximize $\|\nabla g^{x_0}\|_{L_1(\tilde{\Omega})}$ over all unit vectors. Experiments indicate that we should choose $\boldsymbol{\nu}$ as the unit eigenvector corresponding to the smallest eigenvalue of $\tilde{A}_h^{x_0}$, which is $e_1 = (1, 0)$. Thus all parameters

necessary to compute g^{x_0} are fixed (except the eigenvalues $\lambda^h(x_0)$ and $\Lambda^h(x_0)$).

In order to estimate $\|\nabla g^{x_0}\|_{L_1(\tilde{\Omega})}$ for given $\lambda^h(x_0)$ and $\Lambda^h(x_0)$, we first note that $\Lambda^h(x_0)g^{x_0} \in H_0^1(\tilde{\Omega})$ solves

$$-\operatorname{div}(\bar{A}_h^{x_0} \nabla(\Lambda^h(x_0)g^{x_0})) = \operatorname{div}(\boldsymbol{\nu} \delta_\epsilon^{x_c}) \text{ in } \tilde{\Omega},$$

where $\bar{A}^h(x_0)$ is the diagonal matrix having eigenvalues $\frac{\lambda^h(x_0)}{\Lambda^h(x_0)}$ and 1. That is, $\Lambda^h(x_0)\|\nabla g^{x_0}\|_{L_1(\tilde{\Omega})}$ is a function of the local eigenvalue gap $\frac{\Lambda^h(x_0)}{\lambda^h(x_0)}$. We thus tabulated values of $\Lambda^h(x_0)\|\nabla g^{x_0}\|_{L_1(\tilde{\Omega})}$ as a function of the eigenvalue gap. Estimation of $\Lambda^h(x_0)\|\nabla g^{x_0}\|_{L_1(\tilde{\Omega})}$ and other computations in this work were carried out using the finite element toolbox ALBERT [13]. Using a nonlinear curve fitting routine, it was determined that

$$\hat{w}(x_0) = 5.05 + 3.95 \left(\frac{\Lambda^h(x_0)}{\lambda^h(x_0)} - .899 \right)^{.941} \quad (3.2)$$

approximates experimental values of $\Lambda^h(x_0)\|\nabla g^{x_0}\|_{L_1(\tilde{\Omega})}$ to within 1%. \hat{w} and experimentally calculated values of $\Lambda^h(x_0)\|\nabla g^{x_0}\|_{L_1(\tilde{\Omega})}$ are displayed in Figure 3.1. Finally, we define

$$w(x_0) = \frac{1}{\Lambda^h(x_0)} \hat{w}(x_0) \quad (3.3)$$

and

$$W(T) = \max_{x_0 \in T} w(x_0).$$

Our estimator for $\|\nabla(u - u_h)\|_{L_\infty(\Omega)}$ is then

$$E_\infty = C(r) \max_{T \in \mathcal{T}} W(T) \mathcal{E}_T.$$

Note that (3.3) implies that

$$w(x_0) \leq \frac{C(\Omega, \epsilon)}{\lambda_h(x_0)}. \quad (3.4)$$

Indeed, as $\epsilon \rightarrow 0$, the exponent in (3.2) (which is .941 for $\epsilon = 10^{-5}$) is seen to increase to 1 in experiments. It is therefore justified to instead define $W(T) = C \max_{x_0 \in T} \frac{1}{\lambda^h(x_0)}$. While more convenient and perhaps better justified theoretically, in test cases this expression appears to lead to some overestimation of the error when $\|\frac{\Lambda^h}{\lambda^h}\|_{L_\infty(\Omega)}$ is large.

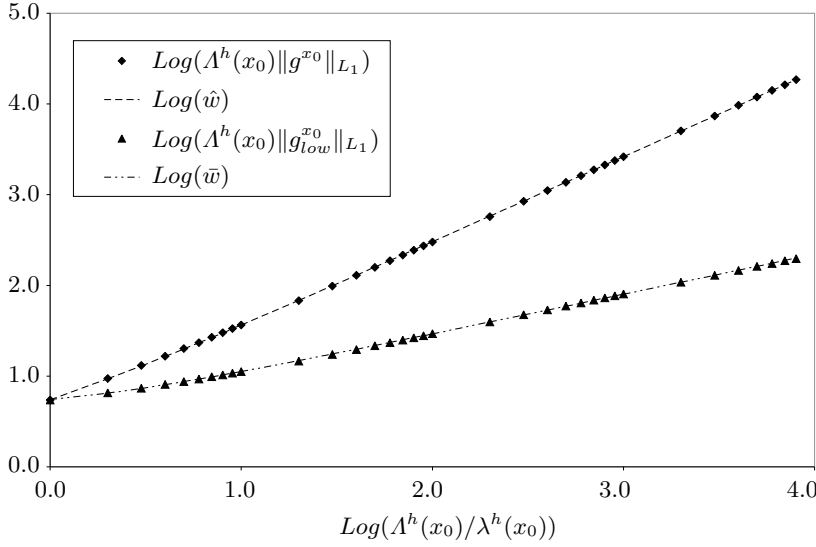


Fig. 3.1. Estimation of regularized Green's functions used in the definitions of $W(T)$.

While the function $w(x_0)$ depends on the domain $\tilde{\Omega} = [0, 1] \times [0, 1]$, it should not be necessary to recompute w for other domains. In test computations, we for example computed several values of $w(x_0)$ on a hexagonal domain and found them to be nearly identical to those computed on $\tilde{\Omega}$ above. While we do not attempt to theoretically justify such an assertion, it appears that values of $w(x_0)$ on two different domains differ only by a constant depending on the domains.

Finally, we note that it is possible to define and compute analogous weights when the space dimension $n > 2$. We do not give the details here.

3.2 *A posteriori* lower bounds and the eigenvalue gap

To begin our discussion of *a posteriori* lower bounds, we recall from (1.2) that $\frac{1}{\Lambda_{S_T}^h} \mathcal{E}_T \lesssim \|\nabla(u - u_h)\|_{L_\infty(S_T)} + R_1(S_T)$. Neglecting higher-order terms, assuming that $\|\nabla(u - u_h)\|_{L_\infty(\Omega)} \lesssim \max_{T \in \mathcal{T}} W(T) \mathcal{E}_T$, and taking a maximum over $T \in \mathcal{T}$ thus yields a gap between a *a posteriori* upper and lower bounds of

$$\max_{T \in \mathcal{T}} \Lambda_{S_T}^h W(T) = \max_{x_0 \in \Omega} \Lambda^h(x_0) \|g^{x_0}\|_{L_1(\tilde{\Omega})} + R(\Omega).$$

$\Lambda^h(x_0)\|g^{x_0}\|_{L_1(\tilde{\Omega})} \approx \hat{w}(x_0)$ is the quantity plotted in the upper curve in Figure 3.1 and grows approximately as $(\frac{\Lambda^h(x_0)}{\lambda^h(x_0)})^{.941}$. Thus the gap (up to higher-order terms) between a posteriori upper and lower bounds grows slightly sublinearly with respect to the maximum pointwise eigenvalue gap. Stated more simply, this gap is about $\|\frac{\Lambda^h}{\lambda^h}\|_{L_\infty(\Omega)}$. In §5 we give computational experiments which confirm the sharpness of these bounds by showing that the actual error may closely track either the a posteriori upper or lower bound.

Recall that g^{x_0} was defined by maximizing $\|\nabla g^{x_0}\|_{L_1(\tilde{\Omega})}$ over possible choices of the unit vector ν in (3.1). As mentioned above, the best choice of the direction ν from theoretical considerations would be $\nabla(u - u_h)/|\nabla(u - u_h)|$. This might lead one to guess that *minimizing* $\|\nabla g^{x_0}\|_{L_1(\tilde{\Omega})}$ over possible choices of ν could lead to an a posteriori lower bound, but this is not the case. We define an alternate regularized Green's function $g_{low}^{x_0}$ by choosing $\nu = e_2$, which minimizes $\|\nabla g_{low}^{x_0}\|_{L_1(\tilde{\Omega})}$ over unit vectors ν . Then with $\bar{w}(x_0) = .365 + 3.77(\frac{\Lambda^h(x_0)}{\lambda^h(x_0)} + 1.02)^{.441}$,

$$\tilde{w}(x_0) = \frac{1}{\Lambda^h(x_0)}\bar{w}(x_0)$$

approximates experimental values of $\|\nabla g_{low}^{x_0}\|_{L_1(\tilde{\Omega})}$ to within about 1%. $\bar{w}(x_0)$ and experimental values of $\Lambda^h(x_0)\|\nabla g_{low}^{x_0}\|_{L_1(\tilde{\Omega})}$ are plotted in Figure 3.1. There is therefore a gap of about $(\frac{\Lambda^h}{\lambda^h})^{.5}$ between $\tilde{w}(x_0)$ and the theoretically justified and experimentally confirmed weight $\frac{1}{\Lambda_T^h}$ for the lower bound. Thus even if we could somehow make a better local choice of the direction ν , we still would be left with a significant eigenvalue gap between the upper and lower bound.

4 Justification of the weight $W(T)$

In this section we first prove a theorem showing that a weight closely related to $W(T)$ yields a reliable upper bound for $\|\nabla(u - u_h)\|_{L_\infty(\Omega)}$ up to higher-order terms and constants not depending on essential quantities. We then argue that this rigorously justifiable but computationally inconvenient estimator may be bounded by E_∞ up to a logarithmic factor.

4.1 A rigorous estimator

In this subsection we show that $\|\nabla(u - u_h)\|_{L^\infty(\Omega)}$ may be estimated up to higher-order terms by a weighted residual estimator where the weights are closely related to $W(T)$. Note that the theoretical results of this subsection are valid for space dimension $n \geq 2$.

Before stating our theorem, we first define a regularized Green's function which will serve as our modified elementwise weight. Given $T \in \mathcal{T}$, let x_T and ν_T be as in Lemma 2.3, and let \tilde{x}_T be the image of x_T under the natural transformation from the subdomain $D_d(x_T)$ defined in §2.3 to $\tilde{\Omega}$. Let then $\tilde{g}^T \in H_0^1(\tilde{\Omega})$ solve

$$-\operatorname{div}(A_h^{x_T} \tilde{g}^{x_T}) = \operatorname{div}(\nu_T \delta_{\tilde{\rho}}^{\tilde{x}_T}) \text{ in } \tilde{\Omega}, \quad (4.1)$$

where $\tilde{\rho}$ is defined below.

Theorem 4.1 *Assume that $u \in C^{1,\alpha}(\bar{\Omega})$ for some $0 < \alpha \leq 1$ and that $\|\nabla u_h\|_{L^\infty(\Omega)} \lesssim 1 + \|\nabla u\|_{L^\infty(\Omega)}$. Then for any $\beta \geq 2$,*

$$\begin{aligned} \|\nabla(u - u_h)\|_{L^\infty(\Omega)} &\lesssim C(r) \max_{T \in \mathcal{T}} (\max_{T' : T \in \mathcal{T}_{D_d(x_{T'})}} \|\nabla \tilde{g}^{T'}\|_{L_1(\tilde{\Omega})}) \mathcal{E}_T \\ &\quad + (C_1)^2 (C_1 \ell_{\underline{h},\beta} |A|_{C^{0,\alpha}(\bar{\Omega})})^{\frac{1}{\alpha}} \ell_{\underline{h},\beta} \|u - u_h\|_{L^\infty(\Omega)} \\ &\quad + C_1 C_F \ell_{\underline{h},\beta} \|\nabla(u - u_h)\|_{L^\infty(\Omega)}^2 \\ &\quad + \underline{h}^{\alpha\beta} |u|_{C^{1,\alpha}(\bar{\Omega})}. \end{aligned} \quad (4.2)$$

Here C_1 depends upon r , \mathbf{F} , and in the nonlinear case on $\|\nabla u\|_{L^\infty(\Omega)}$; $\ell_{\underline{h},\beta} = \max(1, (\beta \ln \frac{1}{\underline{h}})^{\gamma(n)})$ where $\gamma(2) = 2$ and $\gamma(n) = 1$ for $n > 2$; and

$$d = \left(\frac{\mu}{C_1 \ell_{\underline{h},\beta} |A|_{C^{0,\alpha}(\bar{\Omega})}} \right)^{\frac{1}{\alpha}} \quad (4.3)$$

where μ depends on C_T , $\tilde{\Omega}$, and n . Also, $\tilde{\rho} = \min(\frac{\underline{h}^\beta}{d}, \frac{\operatorname{diam}(\tilde{\Omega})}{8})$ in (4.1). Finally, $C_F = 0$ in the linear case.

Proof of Theorem 4.1. Much of our proof consists of the following local estimate.

Lemma 4.1 *Let the conditions of Theorem 4.1 be satisfied. Then for any $T \in \mathcal{T}$,*

$$\begin{aligned} \|\nabla(u - u_h)\|_{L^\infty(T)} &\lesssim C(r) \|\nabla \hat{g}^T\|_{L_1(D_d(x_T))} [\max_{T' \in \mathcal{T}_{D_d(x_T)}} \mathcal{E}_{T'} \\ &\quad + \frac{\Lambda^h(x_T)}{d} \|u - u_h\|_{L^\infty(D_d(x_T))} + C_F \|\nabla(u - u_h)\|_{L^\infty(\Omega)}^2 \\ &\quad + d^\alpha |A|_{C^{0,\alpha}(\overline{D_d(x_T)})} \|\nabla(u - u_h)\|_{L^\infty(D_d(x_T))}] \\ &\quad + \underline{h}^{\alpha\beta} |u|_{C^{1,\alpha}(\bar{T})}, \end{aligned} \quad (4.4)$$

where $\hat{g}^T \in H_0^1(D_d(x_T))$ solves

$$-\operatorname{div}(A_h^{x_T} \nabla \hat{g}^{x_T}) = \operatorname{div}(\boldsymbol{\nu}_T \delta_\rho^{x_T}) \text{ in } D_d(x_T)$$

with $\rho = d\tilde{\rho} = \min(\underline{h}^\beta, \frac{d \operatorname{diam}(\tilde{\Omega})}{8})$.

Proof of Lemma 4.1. We first apply Lemma 2.3 with ρ as defined above, yielding

$$\|\nabla(u - u_h)\|_{L_\infty(T)} \lesssim |(u - u_h, \partial \delta_\rho^{x_T})| + \underline{h}^{\alpha\beta} |u|_{C^{1,\alpha}(\bar{T})}, \quad (4.5)$$

where $\partial v = \nabla v \cdot \boldsymbol{\nu}_T$ as in Lemma 2.3. Recalling from §2.3 the definition of the cutoff function ω associated to x_0 , we compute

$$\begin{aligned} (u - u_h, \partial \delta_\rho^{x_T}) &= (\omega(u - u_h), \partial \delta_\rho^{x_T}) \\ &= \int_{D_d(x_T)} A_h^{x_T} \nabla(\omega(u - u_h)) \cdot \nabla \hat{g}^T \, dx \\ &= \int_{D_d(x_T)} A_h^{x_T} \nabla(u - u_h) \cdot \nabla(\omega \hat{g}^T) \, dx \\ &\quad + \int_{D_d(x_T)} (u - u_h) A_h^{x_T} \nabla \omega \nabla \hat{g}^T \, dx \\ &\quad - \int_{D_d(x_T)} \hat{g}^T A_h^{x_T} \nabla(u - u_h) \cdot \nabla \omega \, dx \\ &= \int_{D_d(x_T)} A_h^{x_T} \nabla(u - u_h) \cdot \nabla(\omega \hat{g}^T) \, dx \\ &\quad + \int_{D_d(x_T)} (u - u_h) A_h^{x_T} \nabla \omega \nabla \hat{g}^T \, dx \\ &\quad + \int_{D_d(x_T)} (u - u_h) \operatorname{div}(\hat{g}^T A_h^{x_T} \nabla \omega) \, dx. \end{aligned}$$

The boundary terms in the last integration by parts disappear because $u - u_h = 0$ on $\partial\Omega$ and $\omega = 0$ in a neighborhood of $\partial D_d(x_T) \setminus \partial\Omega$. Recalling that $\|\omega\|_{W_\infty^k(\Omega)} \lesssim d^{-k}$ and using the Poincaré inequality $\|\hat{g}^T\|_{L_1(D_d(x_T))} \leq Cd \|\nabla \hat{g}^T\|_{L_1(D_d(x_T))}$, we thus find that

$$\begin{aligned} |(u - u_h, \partial \delta_\rho^{x_T})| &\lesssim |A_h^{x_T}(u - u_h, \omega \hat{g}^T)| \\ &\quad + \frac{1}{d} A^h(x_T) \|\nabla \hat{g}^T\|_{L_1(D_d(x_T))} \|u - u_h\|_{L_\infty(D_d(x_T))}. \end{aligned} \quad (4.6)$$

Next we calculate as in (3.11) and (3.12) of [4] while recalling (2.3) and noting that $\mathcal{T}_{D^h} = \mathcal{T}_D$ to find

$$\begin{aligned} &A_h(u - u_h, \omega \hat{g}^T - I_h(\omega \hat{g}^T)) \\ &\leq \|\nabla(\omega \hat{g}^T)\|_{L_1(\operatorname{supp}(I_h(\omega \hat{g}^T)))} \max_{T' \in \mathcal{T}_{\operatorname{supp}(I_h(\omega \hat{g}^T))}} \mathcal{E}_{T'} \\ &= \|\nabla(\omega \hat{g}^T)\|_{L_1(D_d(x_T))} \max_{T' \in \mathcal{T}_{D_d(x_T)}} \mathcal{E}_{T'} \end{aligned}$$

We thus apply (2.5) and (2.6) to compute

$$\begin{aligned} &A_h^{x_T}(u - u_h, \omega \hat{g}^T) \\ &= (A_h^{x_T} - A_h)(u - u_h, \omega \hat{g}^T) + A_h(u - u_h, \omega \hat{g}^T - I_h(\omega \hat{g}^T)) \\ &\lesssim C(r) \|\nabla(\omega \hat{g}^T)\|_{L_1(D_d(x_T))} [C_F \|\nabla(u - u_h)\|_{L_\infty(D_d(x_T))}^2 \\ &\quad + d^\alpha |A|_{C^{0,\alpha}(D_d(x_T))} \|\nabla(u - u_h)\|_{L_\infty(D_d(x_T))} \\ &\quad + \max_{T' \in \mathcal{T}_{D_d(x_T)}} \mathcal{E}_{T'}]. \end{aligned} \quad (4.7)$$

Finally we employ a Poincaré inequality and recall that $\|\nabla\omega\|_{L_\infty(\Omega)} \lesssim d^{-1}$ to obtain

$$\begin{aligned} \|\nabla(\omega\hat{g}^T)\|_{L_1(D_d(x_T))} &\lesssim \frac{1}{d}\|\hat{g}^T\|_{L_1(D_d(x_T))} + \|\nabla\hat{g}^T\|_{L_1(D_d(x_T))} \\ &\lesssim \|\nabla\hat{g}^T\|_{L_1(D_d(x_T))}. \end{aligned} \quad (4.8)$$

Combining (4.5), (4.6), (4.7), and (4.8) completes the proof of Lemma 4.1. \square

In order to complete the proof of Theorem 4.1, we note that a simple scaling argument yields $\|\nabla\hat{g}^T\|_{L_1(D_d(x_T))} = \|\nabla\tilde{g}^T\|_{L_1(\tilde{\Omega})}$. Recall that the global minimum and maximum eigenvalues of $[F_{ij}(\cdot, \nabla u_h)]$ and the constant C_G in the Green's function estimates (2.10) and (2.11) depend only on $\tilde{\Omega}$, \mathbf{F} , and $\|\nabla u\|_{L_\infty(\Omega)}$ since $\|\nabla u_h\|_{L_\infty(\Omega)} \lesssim 1 + \|\nabla u\|_{L_\infty(\Omega)}$. Using an argument similar to that given in [4], Lemma 3.8, we thus find that

$$\|\nabla\hat{g}^T\|_{L_1(D_d(x_T))} = \|\nabla\tilde{g}^T\|_{\tilde{\Omega}} \leq C_1\ell_{\underline{h},\beta} \quad (4.9)$$

and

$$\Lambda^h(x_T) \leq C_1, \quad (4.10)$$

where C_1 depends on C_G and thus only on \mathbf{F} and $\|\nabla u\|_{L_\infty(\Omega)}$.

Inserting (4.9) and (4.10) into (4.4) then yields that for any $T \in \mathcal{T}$,

$$\begin{aligned} \|\nabla(u - u_h)\|_{L_\infty(T)} &\lesssim C(r)\|\nabla\tilde{g}^T\|_{L_1(\tilde{\Omega})} \max_{T \in \mathcal{T}_{D_d(x_T)}} \mathcal{E}_T \\ &\quad + C_1\ell_{\underline{h},\beta} \left[\frac{C_1}{d} \|u - u_h\|_{L_\infty(D_d(x_T))} + C_F \|\nabla(u - u_h)\|_{L_\infty(\Omega)}^2 \right. \\ &\quad \left. + d^\alpha |A|_{C^{0,\alpha}(\overline{D_d(x_T)})} \|\nabla(u - u_h)\|_{L_\infty(D_d(x_T))} \right] \\ &\quad + \underline{h}^{\alpha\beta} |u|_{C^{1,\alpha}(\overline{T})}. \end{aligned}$$

Taking a maximum over $T \in \mathcal{T}$, rearranging terms, and recalling (4.3) yields

$$\begin{aligned} &\|\nabla(u - u_h)\|_{L_\infty(\Omega)} \\ &\lesssim \max_{T \in \mathcal{T}} \|\nabla\tilde{g}^T\|_{L_1(\tilde{\Omega})} (\max_{T' \in \mathcal{T}_{D_d(x_T)}} \mathcal{E}_{T'}) \\ &\quad + C_1\ell_{\underline{h},\beta} \left[\frac{C_1}{d} \|u - u_h\|_{L_\infty(\Omega)} + C_F \|\nabla(u - u_h)\|_{L_\infty(\Omega)}^2 \right] \\ &\quad + C\underline{h}^{\alpha\beta} |u|_{C^{1,\alpha}(\overline{\Omega})} \\ &\quad + C_1\ell_{\underline{h},\beta} d^\alpha |A|_{C^{0,\alpha}(\overline{\Omega})} \|\nabla(u - u_h)\|_{L_\infty(\Omega)} \\ &= \max_{T \in \mathcal{T}} (\max_{T': T \in \mathcal{T}_{D_d(x_{T'})}} \|\nabla\tilde{g}^{T'}\|_{L_1(\tilde{\Omega})}) \mathcal{E}_T \\ &\quad + (C_1)^2 \ell_{\underline{h},\beta} (C_1\ell_{\underline{h},\beta} |A|_{C^{0,\alpha}(\overline{\Omega})})^{\frac{1}{\alpha}} \mu^{-\frac{1}{\alpha}} \|u - u_h\|_{L_\infty(\Omega)} \\ &\quad + C_1 C_F \ell_{\underline{h},\beta} \|\nabla(u - u_h)\|_{L_\infty(\Omega)}^2 \\ &\quad + \underline{h}^{\alpha\beta} |u|_{C^{1,\alpha}(\overline{\Omega})} \\ &\quad + \mu \|\nabla(u - u_h)\|_{L_\infty(\Omega)}. \end{aligned}$$

Taking μ small enough to overcome the nonessential constant hidden in “ \lesssim ” completes the proof of Theorem 4.1. \square

4.2 Heuristic arguments and a final estimate

In this section we first use computational and heuristic evidence to argue that $\|\nabla g^{x_T}\|_{L_1(\tilde{\Omega})}$ bounds $\|\nabla \tilde{g}^T\|_{L_1(\tilde{\Omega})}$ up to a logarithmic factor. The computational evidence we present is valid for the model domain $\tilde{\Omega} = \Omega = (0, 1) \times (0, 1)$, but the same observations are generally valid for other situations as well. We then state and prove a final corollary which may serve as the basis for adaptive mesh refinement algorithms.

First we use computational and heuristic evidence to argue that for $T \in \mathcal{T}$,

$$\|\nabla \tilde{g}^T\|_{L_1(\tilde{\Omega})} \lesssim \hat{\ell}_{h,\epsilon} \|\nabla g^{x_T}\|_{L_1(\tilde{\Omega})}, \quad (4.11)$$

where $\hat{\ell}_{h,\epsilon} = \max(1, \frac{\ell_{h,\beta}}{\ln 1/\epsilon})$. The differences in the data used to define \tilde{g}^T and g^{x_T} are:

1. *The relative location of the regularized δ -distribution within $\tilde{\Omega}$ varies in the definition of \tilde{g}^T but is fixed in the definition of g^{x_T} .* Computational experiments indicate that $\|\nabla g^{x_T}\|_{L_1(\tilde{\Omega})}$ is maximized when the discrete δ -function is placed at the center of the domain as in our definition of $W(T)$. For example, we carried out test computations with $\epsilon = 10^{-3}$ and $\frac{\Lambda^h(x_0)}{\lambda^h(x_0)} = 100$. With $x_c = (.5, .5)$, we obtained $\Lambda^h(x_0)\|\nabla g^{x_0}\|_{L_1(\tilde{\Omega})} = 163$; with $x_c = (.65, .65)$, 160; and with $x_c = (.9975, .9975)$, 27.
2. *The directions ν_T in Theorem 4.1 and ν in §3.1 may differ.* Recall that ν was chosen in order to maximize $\|\nabla g^{x_T}\|_{L_1(\tilde{\Omega})}$.
3. *The coefficient matrices $\tilde{A}_h^{x_T}$ in (3.1) and $A_h^{x_T}$ in (4.1) are different.* $\tilde{A}_h^{x_T}$ and $A_h^{x_T}$ are symmetric and have the same eigenvalues $\lambda_h(x_T)$ and $\Lambda_h(x_T)$, and are thus equivalent up to a rotation of their eigenvectors. Recall that $\tilde{A}_h^{x_T}$ is diagonal, so that its eigenvectors were parallel to the sides of $\tilde{\Omega}$ in our experiments. Redefining $\tilde{A}_h^{x_T}$ so that its eigenvectors had arbitrary orientation with respect to $\tilde{\Omega}$ yielded values for $W(T)$ that were at most a few percent different than those displayed in Figure 3.1.
4. *ϵ is fixed and not equal to $\tilde{\rho}$.* Heuristic theoretical evidence indicates and computational experiments confirm that choosing ϵ reasonably small in the definition of g^{x_T} will ensure that $\|\nabla g^{x_T}\|_{L_1(\tilde{\Omega})}$ grows approximately logarithmically with ϵ , that is, $\|\nabla g^{x_T}\|_{L_1(\tilde{\Omega})} \approx \frac{1}{\Lambda^h(x_T)} C(\Lambda^h(x_T)/\lambda^h(x_T)) \ln \frac{1}{\epsilon}$. For example, if we choose $\epsilon = 10^{-5}$ and $\Lambda^h(x_T)/\lambda^h(x_T) = 1000$, we have $\|\nabla g^{x_T}\|_{L_1(\tilde{\Omega})} \approx 2629$. With $\epsilon = 10^{-6}$ we obtain $\|\nabla g^{x_T}\|_{L_1(\tilde{\Omega})} \approx 3315$, yielding a growth

factor of $\frac{3315}{2629} \approx 1.26$ versus the factor of $\frac{\ln 10^{-6}}{\ln 10^{-5}} = 1.2$ which would result from perfectly logarithmic growth with ϵ . Further experiments show similar results.

Based on these arguments we conclude that (4.11) holds.

Our final result is the following corollary.

Corollary 4.1 *Assume that (4.11) and the conditions of Theorem 4.1 hold. Then*

$$\begin{aligned} \|\nabla(u - u_h)\|_{L^\infty(\Omega)} &\lesssim C(r)\hat{\ell}_{h,\epsilon} \max_{T \in \mathcal{T}} W(T)\mathcal{E}_T \\ &+ (C_1)^2 (C_1 \ell_{h,\beta} |A|_{C^{0,\alpha}(\bar{\Omega})})^{\frac{1}{\alpha}} \ell_{h,\beta} \|u - u_h\|_{L^\infty(\Omega)} \\ &+ C_1 C_F \ell_{h,\beta} (\|\nabla(u - u_h)\|_{L^\infty(\Omega)}^2 + \|w\|_{L^\infty(\Omega)}^2) \max_{T \in \mathcal{T}} \mathcal{E}_T^2 \\ &+ \underline{h}^{\alpha\beta} |u|_{C^{1,\alpha}(\bar{\Omega})}, \end{aligned} \quad (4.12)$$

where $C_F = 0$ in the linear case.

Proof of Corollary 4.1. Most of the proof of (4.12) consists of showing that for $T \in \mathcal{T}$,

$$\begin{aligned} (\max_{T' \in \mathcal{T}_{D_d(x_{T'})}} w(x_{T'}))\mathcal{E}_T &\leq W(T)\mathcal{E}_T \\ &+ C_1 C_F (\|\nabla(u - u_h)\|_{L^\infty(\Omega)}^2 + \|w\|_{L^\infty(\Omega)}^2) \max_{T \in \mathcal{T}} \mathcal{E}_T^2. \end{aligned} \quad (4.13)$$

Assuming (4.13), combining (4.13), (4.2), and (4.11) while noting that $\hat{\ell}_{h,\epsilon} \leq \ell_{h,\beta}$ yields (4.12).

In order to prove (4.13), we begin by fixing an element T' such that $T \in \mathcal{T}_{D_d(x_{T'})}$ and note that there exists a point $x_1 \in T$ such that $|x_{T'} - x_1| \lesssim d$. Then

$$\begin{aligned} w(x_{T'})\mathcal{E}_T &\leq |w(x_{T'}) - w(x_1)|\mathcal{E}_T + w(x_1)\mathcal{E}_T \\ &\leq |w(x_{T'}) - w(x_1)|\mathcal{E}_T + W(T)\mathcal{E}_T. \end{aligned} \quad (4.14)$$

For the sake of notational convenience we let $x_0 = x_{T'}$, $\Lambda_0 = \Lambda^h(x_{T'})$, $\lambda_0 = \lambda^h(x_{T'})$, $\Lambda_1 = \Lambda^h(x_1)$, and $\lambda_1 = \lambda^h(x_1)$. An elementary calculation yields

$$\begin{aligned} |w(x_{T'}) - w(x_1)| &= \left| \frac{\hat{w}(x_0)}{\Lambda_0} - \frac{\hat{w}(x_1)}{\Lambda_1} \right| \\ &\leq \frac{|\hat{w}(x_0) - \hat{w}(x_1)|}{\Lambda_i} + \frac{|\Lambda_1 - \Lambda_0| \hat{w}(x_j)}{\Lambda_0 \Lambda_1}, \end{aligned} \quad (4.15)$$

where $i = 0$ or $i = 1$ is chosen so that $\frac{\Lambda_i}{\lambda_i} = \min(\frac{\Lambda_0}{\lambda_0}, \frac{\Lambda_1}{\lambda_1})$ and $i \neq j \in \{0, 1\}$. Then we note that for some b between $\frac{\Lambda_0}{\lambda_0}$ and $\frac{\Lambda_1}{\lambda_1}$,

$$\begin{aligned} |\hat{w}(x_0) - \hat{w}(x_1)| &= 3.95 \left| \left(\frac{\Lambda_0}{\lambda_0} - .899 \right)^{.941} - \left(\frac{\Lambda_1}{\lambda_1} - .899 \right)^{.941} \right| \\ &= (3.95)(.941)(b - .899)^{-.059} \left| \frac{\Lambda_0}{\lambda_0} - \frac{\Lambda_1}{\lambda_1} \right| \\ &\leq (.941)\hat{w}(x_i) \left(\frac{\Lambda_i}{\lambda_i} - .899 \right)^{-1} \left| \frac{\Lambda_i}{\lambda_i} \frac{\lambda_j - \lambda_i}{\lambda_j} + \frac{\Lambda_i - \Lambda_j}{\lambda_j} \right| \\ &\leq 10\hat{w}(x_i) \frac{|\lambda_1 - \lambda_0| + |\Lambda_1 - \Lambda_0|}{\lambda_j}. \end{aligned} \quad (4.16)$$

The last inequality above follows since $\frac{\Lambda_i}{\lambda_i} \geq 1$. Since $\lambda_j \leq \Lambda_j$, inserting (4.16) into (4.15) yields

$$|w(x_{T'}) - w(x_1)| \lesssim w(x_i) \frac{|\lambda_1 - \lambda_0| + |\Lambda_1 - \Lambda_0|}{\lambda_j} + w(x_j) \frac{|\Lambda_1 - \Lambda_0|}{\Lambda_i}. \quad (4.17)$$

Applying for example Theorem 8.1.4 of [9] and recalling that $|x_0 - x_1| = |x_{T'} - x_1| \leq d$, we next find that

$$\begin{aligned} |\Lambda_1 - \Lambda_0| &= |\Lambda^h(x_1) - \Lambda^h(x_0)| \\ &\leq |\Lambda^h(x_0) - \Lambda(x_0)| + |\Lambda(x_0) - \Lambda(x_1)| + |\Lambda(x_1) - \Lambda^h(x_1)| \\ &\lesssim \|A_h^{x_0} - A^{x_0}\| + \|A(x_0) - A(x_1)\| + \|A^{x_1} - A_h^{x_1}\| \\ &\lesssim C_F(|\nabla(u - u_h)(x_0)| + |\nabla(u - u_h)(x_1)|) + d^\alpha |A|_{C^{0,\alpha}(\bar{\Omega})}. \end{aligned} \quad (4.18)$$

$|\lambda_1 - \lambda_0|$ may be bounded similarly. Noting that $\frac{1}{\lambda_i} + \frac{1}{\Lambda_i} + \frac{1}{\lambda_j} + \frac{1}{\Lambda_j} \leq C_1$, collecting (4.14), (4.17), and (4.18), and inserting (4.3) yields

$$\begin{aligned} w(x_{T'})\mathcal{E}_T &\lesssim C_1 C_F \|\nabla(u - u_h)\|_{L_\infty(\Omega)} (w(x_i) + w(x_j))\mathcal{E}_T \\ &\quad + C_1 |A|_{C^{0,\alpha}(\bar{\Omega})} d^\alpha (w(x_{T'}) + w(x_1))\mathcal{E}_T \\ &\quad + W(T)\mathcal{E}_T \\ &\lesssim C_1 C_F \|\nabla(u - u_h)\|_{L_\infty(\Omega)} \|w\|_{L_\infty(\Omega)} \mathcal{E}_T \\ &\quad + \mu (w(x_{T'}) + w(x_1))\mathcal{E}_T + W(T)\mathcal{E}_T. \end{aligned}$$

Finally we take μ small enough to kick back the term $\mu w(x_{T'})\mathcal{E}_T$ above and also note that $\mu w(x_1)\mathcal{E}_T \leq W(T)\mathcal{E}_T$. Thus

$$\begin{aligned} w(x_{T'})\mathcal{E}_T &\lesssim C_1 C_F \|\nabla(u - u_h)\|_{L_\infty(\Omega)} \|w\|_{L_\infty(\Omega)} \mathcal{E}_T \\ &\quad + W(T)\mathcal{E}_T \\ &\lesssim C_1 C_F (\|\nabla(u - u_h)\|_{L_\infty(\Omega)}^2 + \|w\|_{L_\infty(\Omega)}^2) \max_{T \in \mathcal{T}} \mathcal{E}_T^2 \\ &\quad + W(T)\mathcal{E}_T. \end{aligned} \quad (4.19)$$

Taking a maximum of (4.19) over $T' : T \in \mathcal{T}_{D_d(x_{T'})}$ completes the proof of (4.13). \square

4.3 Discussion of Theorem 4.1 and Corollary 4.1

First we consider (4.2) and (4.12) when the underlying equation is linear, that is, when $\mathbf{F}(x, \nabla u) = A(x)\nabla u(x)$. We will assume that $A \in W_\infty^1(\Omega)$. First we note that with a slight modification to the proof of Theorem 4.1, (4.12) may be reduced to

$$\begin{aligned} \|\nabla(u - u_h)\|_{L_\infty(\Omega)} &\lesssim C(r)\hat{\ell}_{h,\epsilon} \max_{T \in \mathcal{T}} W(T)\mathcal{E}_T \\ &\quad + (C_1)^3 \ell_{h,\beta}^2 |A|_{W_\infty^1(\Omega)} \|u - u_h\|_{L_\infty(\Omega)} \\ &\quad + \underline{h}^{\alpha\beta} |u|_{C^{1,\alpha}(\bar{\Omega})}, \end{aligned}$$

where C_1 depends only on ellipticity properties of A .

Our goal in this work has been to construct an estimator for $\|\nabla(u - u_h)\|_{L_\infty(\Omega)}$ which is reliable up to nonessential constants and higher-order terms. For linear problems, however, the problem of bounding a posteriori the higher order terms which arise is not completely intractable. In [3], the term $\underline{h}^{\alpha\beta}$ was reabsorbed into the left hand side under the nondegeneracy and smoothness assumption that there exists a point $x_1 \in \Omega$ and $\eta > 0$ such that $u \in W_\infty^{r+1}(B_\eta(x_1))$, $\|u\|_{W_\infty^{r+1}(B_\eta(x_1))} \leq C^{**}$, and $|D^r u(x_1)| \geq C^*$. This condition is relatively weak, essentially requiring only that u is sufficiently smooth on a small subdomain of Ω . If in addition u satisfies the regularity estimate $\|u\|_{C^{1,\alpha}(\overline{\Omega})} \leq \|f\|_{L_\infty(\Omega)}$, then the term $\underline{h}^{\alpha\beta}|u|_{C^{1,\alpha}(\overline{\Omega})}$ may be omitted if the logarithmic factors are modified to $\frac{r}{\alpha} \max(\ln \frac{C^{**} + \|f\|_{L_\infty(\Omega)}}{C^*}, \ln \frac{1}{\underline{h}^\beta})$.

If we assume (3.4) and (4.11), tracing the constant C_1^3 above through the proof of Theorem 4.1 yields $C_1^3 \lesssim \ell_h \|\frac{A}{\lambda}\|_{L_\infty(\Omega)} \|\frac{1}{\lambda}\|_{L_\infty(\Omega)}$, where ℓ_h is a generic logarithmic factor. In addition,

$$\|u - u_h\|_{L_\infty(\Omega)} \leq C(A) \ell_h \max_{T \in \mathcal{T}} h_T \mathcal{E}_T; \quad (4.20)$$

cf. [11], [2], and [12]. Here $C(A)$ depends on A in an unknown fashion. Combining the discussion of the preceding two paragraphs, we thus find that under reasonable assumptions,

$$\begin{aligned} \|\nabla(u - u_h)\|_{L_\infty(\Omega)} &\leq C(r) \ell_{h,f,C^*,C^{**}} [\max_{T \in \mathcal{T}} W(T) \mathcal{E}_T \\ &\quad + \|\frac{A}{\lambda}\|_{L_\infty(\Omega)} \|\frac{1}{\lambda}\|_{L_\infty(\Omega)} |A|_{W_\infty^1(\Omega)} C(A) \max_{T \in \mathcal{T}} h_T \mathcal{E}_T], \end{aligned} \quad (4.21)$$

where $\ell_{h,f,C^*,C^{**}}$ is a logarithmic factor depending on the given quantities. If $C(A)$ could be determined with reasonable accuracy, then (4.21) could serve as the basis for an a posteriori estimator for $\|\nabla(u - u_h)\|_{L_\infty(\Omega)}$ which is reliable even on very coarse grids. We emphasize that a chief advantage of (4.21) is that global ellipticity properties of A only appear in higher-order terms. We do not pursue further here the estimation of $C(A)$, a more accurate estimation of the constants in (4.2) or (4.11), or other consideration of the higher-order term in (4.21).

For nonlinear problems the situation is more complex. For a fixed solution u , all terms in (4.2) and (4.12) except the first are of higher order. Theorem 4.1 and Corollary 4.1 are stated so that the constants in these higher-order terms depend on the unknown solution u and are thus noncomputable. As for linear problems, tracing through the proof of Theorem 4.1 yields more information about these constants.

The constant C_1 may always be estimated a posteriori, though we have transformed it into an a priori constant via the assumption $\|\nabla u_h\|_{L^\infty(\Omega)} \lesssim 1 + \|\nabla u\|_{L^\infty(\Omega)}$ in order to ensure that C_1 is fixed independent of the mesh. C_F may be bounded in some situations; $C_F = 1$ for the prescribed mean curvature problem, for example. The treatment of the constant $|A|_{C^{0,\alpha}(\overline{\Omega})}$ is most troublesome. In Lemma 4.1, the term $d^\alpha |A|_{C^{0,\alpha}(\overline{D_d(x_T)})} \|\nabla(u - u_h)\|_{L^\infty(D_d(x_T))}$ may be replaced by $\text{osc}_{D_d(x_T)}[F_{ij}(\cdot, \nabla u_h)] \|\nabla(u - u_h)\|_{L^\infty(D_d(x_T))}$. Thus d must be taken small enough so that $\|\nabla \hat{g}^T\|_{L^1(D_d(x_T))} \text{osc}_{D_d(x_T)}[F_{ij}(\cdot, \nabla u_h)] \leq \mu$, so that we may eventually kick this term back. While estimating d is perhaps possible a posteriori, it appears rather impractical. Finally, as in the linear case the term $\underline{h}^{\alpha\beta} |u|_{C^{1,\alpha}(\overline{\Omega})}$ may be reabsorbed into the left hand side under a suitable nondegeneracy and smoothness condition.

Even if the constants in (4.2) or (4.11) could be accurately estimated, we still would need to bound $\|u - u_h\|_{L^\infty(\Omega)}$ and $\|\nabla(u - u_h)\|_{L^\infty(\Omega)}^2$ a posteriori. If $u \in W_\infty^2(\Omega)$ (which would generally be true if $\partial\Omega$ were smooth, but not in the current situation), then a result similar to (4.20) holds, though still with unaccounted-for terms of yet higher order on the right hand side; cf. [4]. However, we do not know how to estimate the nonlinear perturbation term $\|\nabla(u - u_h)\|_{L^\infty(\Omega)}^2$ a posteriori, except to make the observation that it may be kicked back if $\|\nabla(u - u_h)\|_{L^\infty(\Omega)}$ is small enough to resolve $C_1 C_F$. The assumption that $\|\nabla(u - u_h)\|_{L^\infty(\Omega)}$ is small enough does appear in other a posteriori estimates for quasilinear problems; cf. [15]. In [7], a condition which is verifiable a posteriori (up to an unknown constant) is given. The fulfillment of this condition ensures the reliability of an estimate for a natural geometric norm for the prescribed mean curvature problem, thus removing the necessity of ensuring (or assuming) that $\|\nabla(u - u_h)\|_{L^\infty(\Omega)}$ is small enough.

5 Computational Experiments

In this section we present computational experiments which illustrate both the utility and limitations of the weighted estimator $\max_{T \in \mathcal{T}} W(T)$ in adaptive mesh refinement and a posteriori error estimation.

5.1 Algorithm

First we give the computational algorithm used in our experiments and then make some remarks concerning it. Our adaptive algorithm is:

1. Solve for u_h on an initial uniform mesh \mathcal{T} .
2. For each element $T \in \mathcal{T}$, calculate $W(T)\mathcal{E}_T$.
3. If $E_\infty = C(r) \max_{T \in \mathcal{T}} W(T)\mathcal{E}_T \leq \text{tol}$, stop. If not, continue.
4. Decide which elements of \mathcal{T} should be marked for refinement:
 - (a) For each element $T \in \mathcal{T}$, mark T for refinement if

$$W(T)\mathcal{E}_T \geq \theta \max_{T \in \mathcal{T}} W(T)\mathcal{E}_T. \quad (5.1)$$

- (b) Calculate the percentage P of elements which were marked. If P is less than a given threshold μ , lower θ .
 - (c) Repeat the preceding two steps until $P \geq \mu$.
5. Refine the marked elements to obtain a new mesh \mathcal{T} and calculate a new discrete solution u_h on \mathcal{T} .
6. Return to step 2.

Note that we use a modified version of the standard “maximum strategy” (see e.g. [16]) for deciding which elements to mark for refinement. Our justification for ensuring that a given percentage of elements is marked for refinement at each iteration of the algorithm lies in the conditioning gap between the a posteriori upper and lower bounds for $\|\nabla(u - u_h)\|_{L_\infty(\Omega)}$. From the discussion in §3.2, the weighted elementwise residual $W(T)\mathcal{E}_T$ may overestimate the local error contribution if $\max_{x \in T} \frac{\Lambda^h(x)}{\lambda^h(x)}$ is large. Such overestimation does occur in practice, and on some elements more than on others. Thus in our calculations it sometimes happened that only a few elements were marked for refinement when a typical value for θ was used (we took $\theta = .25$ in most calculations, e.g.). In these cases, ensuring that a given percentage (typically 2%) of elements was marked for refinement usually yielded a reasonable error reduction after the ensuing mesh refinement. This indicates that the elementwise indicator $W(T)\mathcal{E}_T$ ordered the elementwise error contributions approximately correctly, even if $W(T)\mathcal{E}_T$ did not always accurately reflect the actual sizes of the elementwise errors.

As in the calculation of the weights $W(T)$, all computations were performed on the domain $\Omega = (0, 1) \times (0, 1)$. Also, quadratic finite elements ($r = 3$) were employed. Next we define the effectivity index

$$I_{eff} = \frac{\|\nabla(u - u_h)\|_{L_\infty(\Omega)}}{E_\infty}.$$

$C(r) = C(3) = .027$ was chosen so that simple model computations with $\mathbf{F}(x, p) = p$ (that is, with the Laplacian) asymptotically yielded an effectivity index of about 1. At each iteration of the algorithm above, $\theta = .25$ was initially chosen and was then sometimes lowered in steps (a), (b), and (c) as stated. The parameter μ was taken to be 2% for calculations where a large local eigenvalue gap was present (Experiments 2 and 3 below) and 0% otherwise (Experiment 1 below). The error threshold tol depended heavily on the problem at hand, and in fact calculations were often simply run until computer resources were exhausted.

Finally note that (4.12) indicates that the error estimator E_∞ is only asymptotically reliable, implying that the grid should be refined sufficiently before beginning the algorithm. Roughly speaking, the grid must resolve the oscillation and ellipticity properties of the coefficient matrix $A = [F_{ij}(\cdot, \nabla u)]$ enough that the higher order terms on the right hand side of (4.12) are sufficiently small. In our tests we found that our algorithm automatically resolved A sufficiently well even starting from very coarse initial grids, at least for quadratic elements. The initial mesh in Step 1 above was thus taken to be a uniform mesh with 4 elements.

5.2 Linear problems

For our computations involving linear test problems, we first define a family of solutions

$$u(x, y) = \sin(\pi\kappa_x x) \sin(\pi\kappa_y y),$$

where κ_x and κ_y are positive integers.

Experiment 1: Isotropic coefficient matrix. Let

$$a(x, y) = 1 - K \sin(\pi\psi x).$$

Here $0 \leq K < 1$ and $\psi > 0$. Note that if $\psi > .5$, then we have $\min_{(x,y) \in \Omega} a(x, y) = 1 - K$. Consider the model problem: Find $u \in H_0^1(\Omega)$ such that

$$-\operatorname{div}(a\nabla u) = f \text{ in } \Omega,$$

where f is defined by our choice of u and a . Note that here the coefficient matrix is completely isotropic, that is, there is no local eigenvalue gap. Thus the gap between the a posteriori upper and lower bounds obtained using $\max_{T \in \mathcal{T}} W(T)\mathcal{E}_T$ and $\max_{T \in \mathcal{T}} \frac{1}{A_T}\mathcal{E}_T$ is asymptotically 1 for this problem, and the estimator E_∞ should closely predict the actual error on sufficiently refined meshes. K and

ψ were varied in order to study the effects of the ellipticity properties and oscillation of a , respectively, on refinement algorithms using E_∞ . In addition, we carried out adaptive mesh refinement using the unweighted indicator $\hat{E}_\infty = \hat{C}(r) \max_{T \in \mathcal{T}} \mathcal{E}_T$ for comparison. Results are displayed in Figure 5.1. Plots of the resulting errors and effectivity indices I_{eff} are shown in Figure 5.1 and Figure 5.2, respectively.

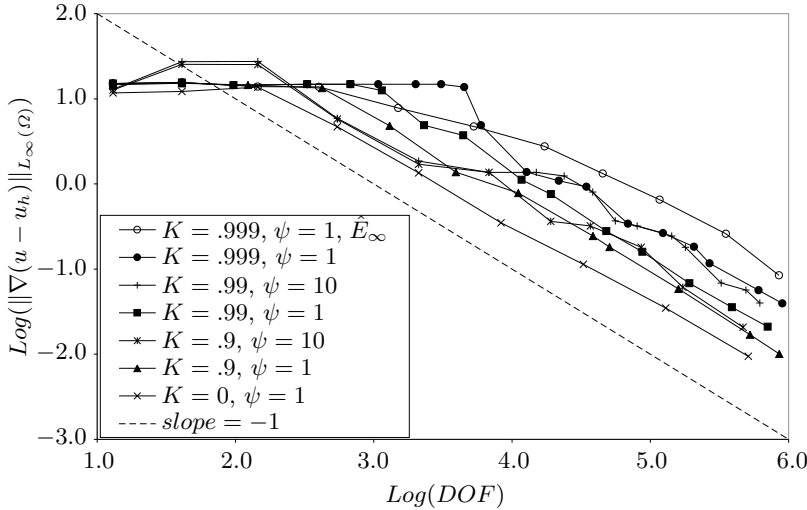


Fig. 5.1. Error reduction achieved for various values of K and ψ in Experiment 1.

We remark on several features of Figure 5.1 and Figure 5.2. First note that the performance of E_∞ as an error indicator is sensitive both to the ellipticity properties and to the oscillation of a . In particular, more degrees of freedom are required to reach a given error tolerance for smaller λ_Ω (larger K in our experiments) and larger oscillation (larger ψ in our experiments). Our experiments thus confirm the validity of the qualitative structure of the estimates (4.12) and (4.21), though not the precise nature of the higher-order terms involved. Secondly, note from Figure 5.2 that the effectivity index I_{eff} asymptotically becomes close to 1 whenever E_∞ is used (though there is no indication that I_{eff} asymptotically tends to 1 or any other constant). Note that when a is highly oscillatory ($\psi = 10$ in our experiments), I_{eff} approaches 1 rather more slowly than if a is not oscillatory. Finally, the unweighted estimator \hat{E}_∞ is able to achieve error reduction which is reasonable but not as good as that achieved

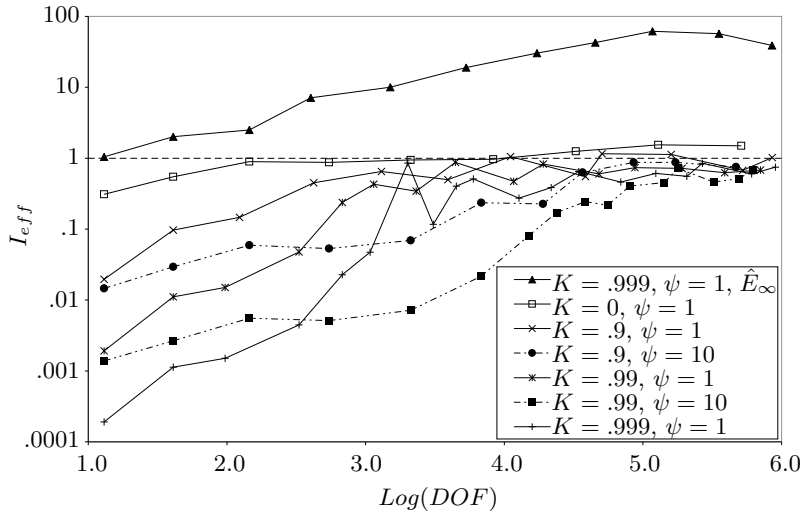


Fig. 5.2. Effectivity indices for Experiment 1.

by E_∞ . In addition, the effectivity index resulting from using \hat{E}_∞ when $\lambda_\Omega = .001$ ($K = .999$) is rather poor.

Experiment 2: Anisotropic coefficient matrix. We tested the effects of an anisotropic coefficient matrix on the performance of E_∞ by letting $u \in H_0^1(\Omega)$ solve

$$-\operatorname{div}(A\nabla u) = f \text{ in } \Omega,$$

where A is a diagonal matrix with $A_{11} = .01$ and $A_{22} = 1$ so that $\|\frac{A}{\lambda}\|_{L_\infty(\Omega)} = 100$. In our calculations we first let $(\kappa_x, \kappa_y) = (20, 1)$ in (5.2). Thus u oscillated heavily in the direction of the eigenvector $(1, 0)$ corresponding to the *smaller* eigenvalue of A and we generally have $\nabla(u - u_h)/|\nabla(u - u_h)| \approx (1, 0)$. Let now $err = \|\nabla(u - u_h)\|_{L_\infty(\Omega)}$ and $e_\infty = C(r) \max_{T \in \mathcal{T}} \frac{1}{\Lambda_T} \mathcal{E}_T$ represent the theoretically justified (up to higher-order terms) lower bound for $\|\nabla(u - u_h)\|_{L_\infty(\Omega)}$. Note that here $e_\infty = C(r) \max_{T \in \mathcal{T}} \mathcal{E}_T$. From Figure 5.3 we see that $err \approx E_\infty$ on sufficiently refined meshes. Also, e_∞ is between 25 and 50 times less than err , which corresponds to the eigenvalue gap of 100 in the coefficient matrix A . Next we let $(\kappa_x, \kappa_y) = (1, 20)$ in (5.2), so that u oscillated heavily in the direction of the eigenvector $(0, 1)$ corresponding to the *larger* eigenvalue of A . Now we observe from Figure 5.3 that asymptotically $err \approx e_\infty$, while E_∞ is between 25 and 50 times greater than err . Thus the sharpness of the upper and lower bounds discussed in §3 is verified.

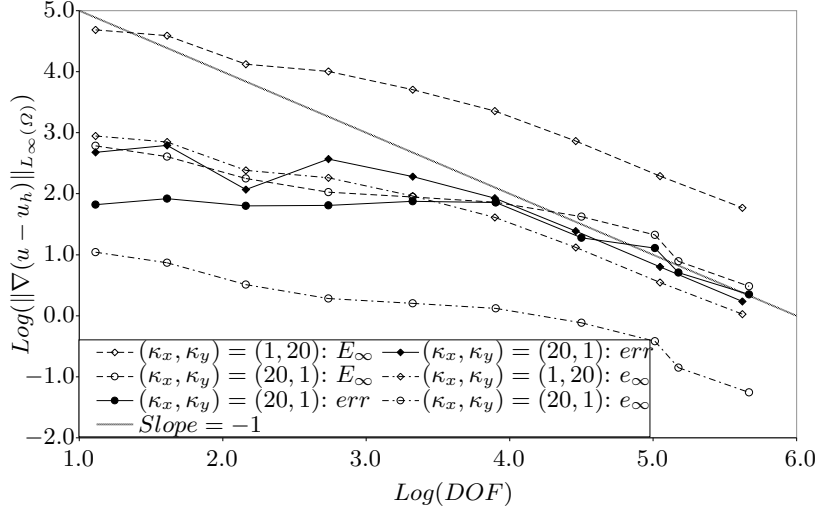


Fig. 5.3. Errors and upper and lower error estimators for Experiment 2.

5.3 Prescribed mean curvature problem

We also tested the effectiveness of our weighting scheme for the nonlinear prescribed mean curvature problem. With $B > .5$, let

$$u_B(x, y) = 3(\sqrt{B^2 - (x - .5)^2} - \sqrt{B^2 - .25}) \cdot (\sqrt{B^2 - (y - .5)^2} - \sqrt{B^2 - .25}).$$

Let $Q = \sqrt{1 + |\nabla u_B|^2}$. Note that as $B \rightarrow .5^+$, $Q_{max} = \|Q\|_{L_\infty(\Omega)} \rightarrow \infty$. Note also that the eigenvalues of $A(x)$ are $\frac{1}{Q}$ and $\frac{1}{Q^3}$, so the local eigenvalue gap is $Q(x)^2$. Thus we predict a conditioning gap of Q_{max}^2 between a posteriori upper and lower bounds E_∞ and e_∞ .

Experiment 3: Nonlinear problem. In our experiments we took $B = .55$ (so that $Q_{max} = 2.33$ and $\|\frac{A}{\lambda}\|_{L_\infty(\Omega)} \approx 5$), $B = .51$ ($Q_{max} = 6.2$ and $\|\frac{A}{\lambda}\|_{L_\infty(\Omega)} \approx 38$), $B = .501$ ($Q_{max} = 22.3$ and $\|\frac{A}{\lambda}\|_{L_\infty(\Omega)} \approx 497$), and $B = .5001$ ($Q_{max} = 73.5$ and $\|\frac{A}{\lambda}\|_{L_\infty(\Omega)} \approx 5230$). Also, for comparison we carried out adaptive mesh refinement using the unweighted error estimator $\hat{E}_\infty = \hat{C}(r) \max_{T \in \mathcal{T}} \mathcal{E}_T$. The resulting error reduction is displayed in Figure 5.4, and efficiency indices are displayed in Figure 5.5.

Marking using the unweighted elementwise indicator \mathcal{E}_T was somewhat effective, but became less so as Q_{max} was increased and was

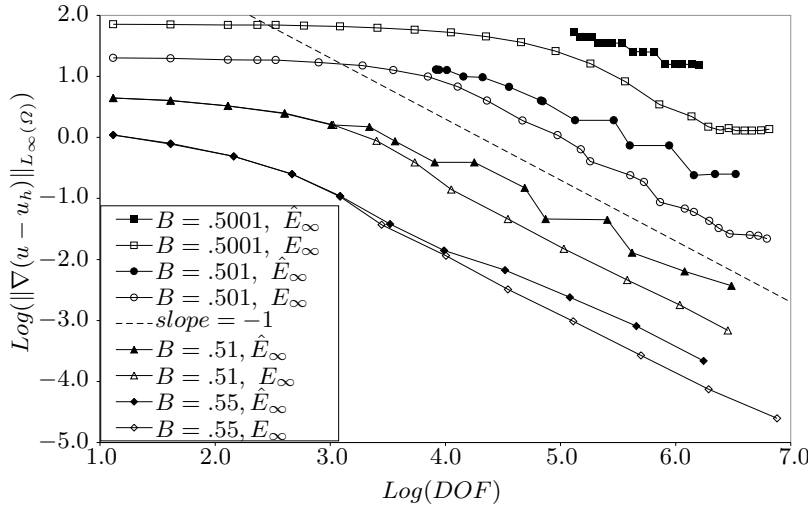


Fig. 5.4. Errors arising from estimation of u_B using indicators E_∞ and \hat{E}_∞ .

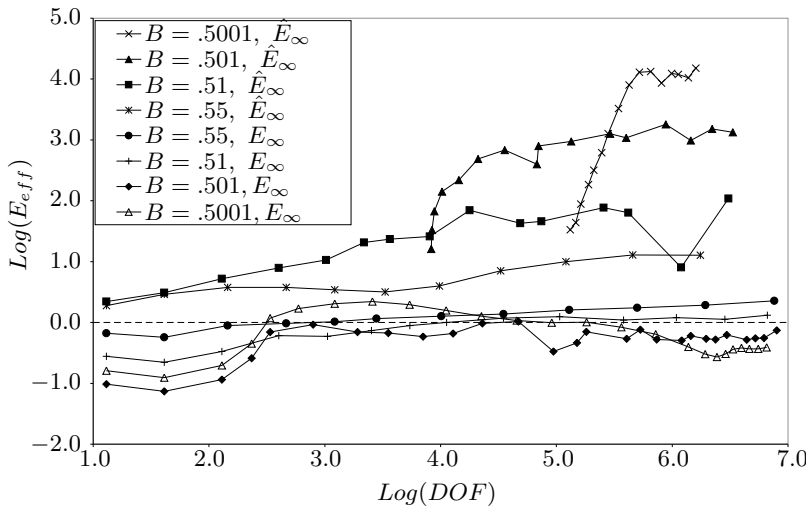


Fig. 5.5. Effectivity indices arising from estimation of u_B using E_∞ and \hat{E}_∞ .

always less effective than using the weighted indicator E_∞ . In addition, Figure 5.5 shows that I_{eff} degenerates very badly as Q_{max} increases. For moderate values of Q_{max} , marking using the weighted indicator $W(T)\mathcal{E}_T$ usually resulted in optimal or nearly-optimal error reduction after a sufficient number of initial refinements. The only

exception occurred when $B = .5001$, where a significant reduction in $\|\nabla(u - u_h)\|_{L^\infty(\Omega)}$ was first achieved (from about 70 to 1.35) and then the algorithm stalled after reaching about 3×10^6 degrees of freedom. In this case performance could be improved somewhat by requiring that the algorithm mark 5% of elements at each iteration rather than 2%, but the resulting error reduction was still sub-optimal with respect to the number of degrees of freedom. Thus the large “eigenvalue gap” present in this problem severely inhibits the performance of the elementwise error indicator $W(T)\mathcal{E}_T$.

From Figure 5.5, we note that E_∞ gives a reliable a posteriori upper bound for all values of B . From Experiment 2 it is clear that this bound may become very pessimistic if the maximum pointwise eigenvalue gap is large, but in the current situation E_∞ performs fairly well as an error estimator even though the eigenvalue gap is large.

References

1. C. BERNARDI AND R. VERFÜRTH, *Adaptive finite element methods for elliptic equations with non-smooth coefficients*, Numer. Math., 85 (2000), pp. 579–608.
2. E. DARI, R. G. DURÁN, AND C. PADRA, *Maximum norm error estimators for three-dimensional elliptic problems*, SIAM J. Numer. Anal., 37 (2000), pp. 683–700 (electronic).
3. A. DEMLOW, *Local a posteriori estimates for pointwise gradient errors in finite element methods for elliptic problems*, Preprint, Fakultät für Mathematik und Physik, Universität Freiburg, (2004).
4. ———, *Localized pointwise a posteriori estimates for gradients of piecewise linear finite element approximations to second-order quasilinear elliptic problems*, Preprint, Fakultät für Mathematik und Physik, Universität Freiburg, (2004).
5. G. DOLZMANN AND S. MÜLLER, *Estimates for Green’s matrices of elliptic systems by L^p theory*, Manuscripta Math., 88 (1995), pp. 261–273.
6. W. DÖRFLER AND O. WILDEROTTER, *An adaptive finite element method for a linear elliptic equation with variable coefficients*, ZAMM Z. Angew. Math. Mech., 80 (2000), pp. 481–491.
7. F. FIERRO AND A. VEESER, *On the a posteriori error analysis for equations of prescribed mean curvature*, Math. Comp., 72 (2003), pp. 1611–1634 (electronic).
8. J. FREHSE AND R. RANNACHER, *Asymptotic L^∞ -error estimates for linear finite element approximations of quasilinear boundary value problems*, SIAM J. Numer. Anal., 15 (1978), pp. 418–431.
9. G. H. GOLUB AND C. F. VAN LOAN, *Matrix computations*, Johns Hopkins Studies in the Mathematical Sciences, Johns Hopkins University Press, Baltimore, MD, third ed., 1996.
10. M. GRÜTER AND K.-O. WIDMAN, *The Green function for uniformly elliptic equations*, Manuscripta Math., 37 (1982), pp. 303–342.

11. R. H. NOCHETTO, *Pointwise a posteriori error estimates for elliptic problems on highly graded meshes*, Math. Comp., 64 (1995), pp. 1–22.
12. R. H. NOCHETTO, A. SCHMIDT, K. G. SIEBERT, AND A. VEESER, *Pointwise a posteriori error estimates for monotone semilinear problems*, In preparation.
13. A. SCHMIDT AND K. G. SIEBERT, *ALBERT—software for scientific computations and applications*, Acta Math. Univ. Comenian. (N.S.), 70 (2000), pp. 105–122.
14. L. R. SCOTT AND S. ZHANG, *Finite element interpolation of nonsmooth functions satisfying boundary conditions*, Math. Comp., 54 (1990), pp. 483–493.
15. R. VERFÜRTH, *A posteriori error estimates for nonlinear problems. Finite element discretizations of elliptic equations*, Math. Comp., 62 (1994), pp. 445–475.
16. ———, *A posteriori error estimation and adaptive mesh-refinement techniques*, in Proceedings of the Fifth International Congress on Computational and Applied Mathematics (Leuven, 1992), vol. 50, 1994, pp. 67–83.